Journal of Engineering and Applied Sciences 14 (5): 1571-1579, 2019
ISSN: 1816-949X

The Study of Corrosion Depth on Lateral Buckling Behavior of High Temperature or High Pressure Subsea Pipeline Induced by Beam Trawl Pull-Over Loads

[1]J.W. Ng, [1]M.A.A. Rahman, [2]E.H. Kasiman and [1]M.H. Mohd
[1]School of Ocean Engineering, Universiti Malaysia Terengganu, 21030 Kuala Nerus, Terengganu, Malaysia
[2]Faculty of Civil Engineering, Universiti Teknologi Malaysia, 81310 Skudai, Johor, Malaysia

Abstract: Subsea pipeline can always relate to corrosion. Different extends of corrosion, making pipeline behaviors unpredictable. It is vulnerable to damages due to the fishing trawl gears and most of the buckling problems are caused by impact and pull-over loads especially the most common practice of using beam trawl. In this research, finite element analysis Abaqus/CAE 6.13-1 was used to study the effect of maximum allowable operating pressure for flawed pipe relates to lateral buckling behavior of straight unburied pipelines on flat clay seabed induced by beam trawl pull-over loads with the usage of different types of steel grade. The primary purpose of this research is to provide a better description of various corrosion depth parameters incorporated with beam trawl pull-over loads and to examine the differences in usage of steel on their performance.

Key words: Subsea pipeline, trawl, performance, vulnerable, lateral buckling, Abaqus/CAE 6.13-1

INTRODUCTION

Each year, corrosion issues on subsea pipelines have been brought up to a high concern of organizations as it brings hazardous to environments especial for oil transmission pipeline. International Association of Oil and Gas Producers (OGP) in 2010 had concluded that corrosion as the second and material as the third main failure mechanism for pipelines (Anonymous, 2010a, b). Lateral buckling occurs under axial compressive loadings accompanied by gradual sideways movement as the unburied pipeline breaks-out to lower the buildup axial compressive force along the pipelines. It is commonly occur for unburied pipelines and the magnitude of 'snaking' is depending on the axial compressive force due to pipe-soil interaction, operational temperature and pressure of pipelines (Khair *et al*., 2015; Guo *et al*., 2013). Beam trawl is where the trawl towed on the seabed in which the net is held open by a rigid framework ensuring it maintains its shape and effectiveness despite changes in towing speed (Montgomerie, 2011). When the bottom trawl is pulled over pipeline, the pipeline may be subjected to relatively large horizontal and vertical forces. For pipelines subjected to beam trawl, only lateral forces exerted on the pipelines. Pipeline will experiences the largest lateral forces at time when the beam trawl going to detach from pipeline and zero forces execute on the pipeline after the beam trawl detach. Therefore, trawl pull-over loads may trigger lateral displacement and associated bending of the pipeline. In combination with the compressive axial force, trawl pull-over may lead to rather large unexpected deflections which are hard to detect earlier (Anonymous, 2010a, b).

Therefore, the aim of this research is to identify the maximum allowable operating pressure at various usage of steel grade and its effects of beam trawl pull-over loads on HT/HP subsea pipelines. Furthermore, the effects of corrosion depth on lateral buckling behavior induced by beam trawl pull-over HT/HP pipelines are also been studied.

MATERIALS AND METHODS

According to ASME B31 code for pressure piping, a standard for maximum allowable operating pressure was recommended in actual practice. Equation 1 can be used for determine maximum allowable operating pressure of non-flawed pipelines:

$$P = \frac{2StFET}{D} \quad (1)$$

Where:
S = Yield Strength (Pa)
t = Thickness of pipe (m)
F = Design Factor
E = Longitudinal joint factor
T = Temperature de-rating factor
D = Outer Diameter (m)

Corresponding Author: M.H. Mohd, School of Ocean Engineering, Universiti Malaysia Terengganu, 21030 Kuala Nerus, Terengganu, Malaysia

Table 1: Design Factor, F (McAllister, 2013)

Construction type (841.151)	Design Factor (F)
A	0.72
B	0.60
C	0.50
D	0.40

Table 2: Longitudinal joint factor for API 5L seamless pipe class, E (McAllister, 2013)

Spec. No.	Pipe class	E factor
ASTM A53	Seamless	1.00
	Electric resistance welded	1.00
	Furnace welded	0.60
ASTM A106	Seamless	1.00
ASTM A134	Electric fusion arc welded	0.80
ASTM A135	Electric resistance welded	1.00
ASTM A139	Electric fusion welded	0.80
ASTM A211	Spiral welded steel pipe	0.80
ASTM A381	Double submerged arc welded	1.00
ASTM A671	Electric fusion welded	1.00
ASTM A672	Electric fusion welded	1.00
API 5L	Seamless	1.00
	Electric resistance welded	1.00
	Electric flash welded	1.00
	Submerged arc welded	1.00
	Furnace butt welded	0.60
API 5LX	Seamless	1.00
	Electric resistance welded	1.00
	Electric flash welded	1.00
	Submerged arc welded	1.00
API 5LS	Electric resistance welded	1.00
	Submerged welded	1.00

Table 3: Temperature derating factor, T, for steel pipe (McAllister, 2013)

Temperature (°F)	Temperature derating factor T
250 or less	1.000
300	0.967
350	0.933
400	0.900
450	0.867

In determine the maximum allowable operating pressure of flawed pipelines, Eq. 2 can be used (Table 1-3):

$$P' = 1.1P\left[1-\frac{d}{t}\right] \quad (2)$$

Where:

P = Max allowable operating pressure for non-flawed pipe (Pa)

d = Depth of defect (m)

Beam trawl pull-over analysis: The standard used for pull-over analysis is based on DNV-OS-F101, DNV-RP-F110 and DNV-RP-F111 (Anonymous, 2010a, b 2007, 2013).

Maximum horizontal load: The maximum horizontal force applied to pipe model is given by Anonymous (2010a, b): beam trawls:

$$F_p = C_F.V\left[(m_t+m_a).k_w\right]^{\frac{1}{2}} \quad (3)$$

where, beam trawl with hoop bars empirical coefficient, C_F, is defined as:

$$C_F = \begin{cases} 4.0 & OD/H_a<2 \\ 6.0\text{-}OD/H_a \text{ for } 2<OD/H_a<3 \\ 3.0 & OD/H_a>3 \end{cases} \quad (4)$$

Beam trawls without hoop bars empirical coefficient, C_F is defined as:

$$C_F = \begin{cases} 5.0 & CD/H_a<2 \\ 8.0\text{-}1.5OD/H_a \text{ for } 2<OD/H_a<3 \\ 3.5 & OD/H_a>3 \end{cases} \quad (5)$$

Where:

m_t = The steel mass of board or beam with shoes

m_a = Hydrodynamic added mass and mass of entrained water

H_a = Attachment point of the warp line, set to 0.2 m

k_w = The warp line stiffness = 3.5, $10^7/L_W$

L_w = Length of the warp line (2.5-3.5 times the water depth). The wire length is relatively longer in shallow water (i.e., 2.5 times is for deep water applications)

V = The tow velocity

Pull-over duration: The total pull-over time is given by Anonymous (2010a, b):

$$T_p = C_T C_F (m_t/k_w)^{\frac{1}{2}} + \delta_p/V \quad (6)$$

Where:

$$\delta_p \approx 0.1(C_T C_F (m/k)^{\frac{1}{2}})$$

C_T = Coefficient for the pullover duration given as: C_T = 1.5 for beam trawls. Since, the value of δ_p/V is unknown, it is assumed that $\delta_p/V = C_T C_F (m/k_w)^{1/2}/10$ in the analysis as recommend by DNV-RP-F111. Hence, the total pull-over time, T_p, equation becomes:

$$T_p = C_T C_F (m_t/k_w)^{\frac{1}{2}} (1+0.1) \quad (7)$$

Numerical analysis: In this research, there are five case studies which is no corrosion, 40% corrosion, 50% corrosion, 60% corrosion and 70% corrosion in depth parameter with the usage of API 5L X42, API 5L X52 and API 5L X65 as shown in Fig. 1. Nonlinear FEA were conducted by using Abaqus/CAE 6.13-1.

Modelling: The models and parts were created in the Abaqus/CAE 6.13-1. There were two parts in a model: pipeline and seabed. For the defect pipelines, the corrosion defect dimension is length of 100.00 mm×width

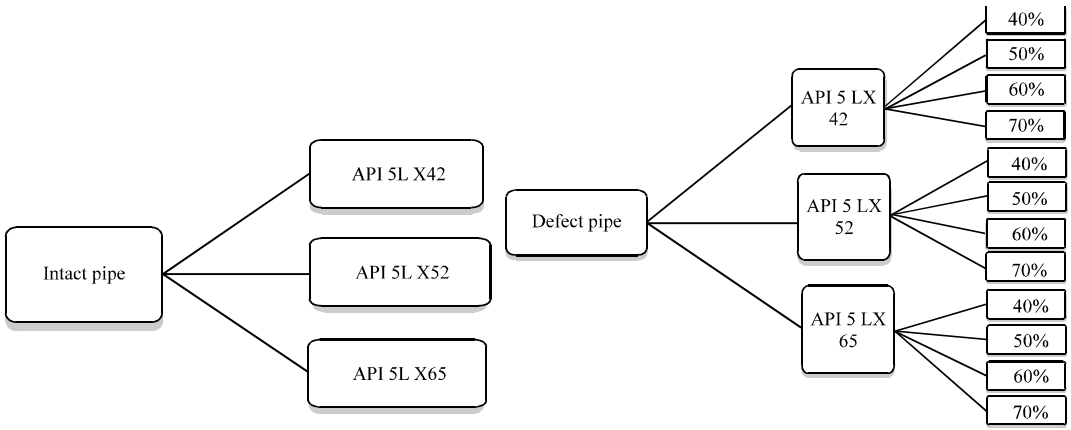

Fig. 1: Case study 1 (no corrosion) and case studies 2-5 (40-70% corrosion)

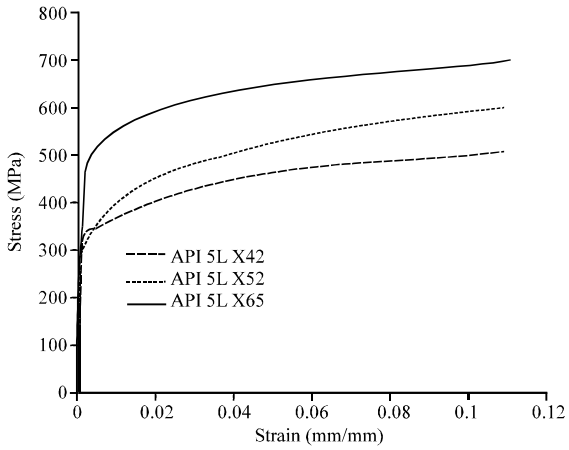

Fig. 2: True stress-strain of steels

of 100.00 mm×depth of 19.05 mm. The length and width of corrosion are constant while the depth of corrosion is varies according to the case study. Details of modeling for both parts were shown as shown in Table 4.

Input data such as density, elastic (Young's Modulus and Poison's ratio), expansion (thermal expansion coefficient) and plasticity (true stress-true strain curve) were inserted into the material property module in Abaqus according to the case study as shown in Table 5, 6 and Fig. 2.

Surface-to-surface contact was selected in assembling pipeline to the center of seabed with master surface (red) of bottom pipe's surface and slave surface (pink) of seabed's surface as shown in Fig. 3. The friction coefficient of seabed and pipeline is 0.5 and the contact stiffness is 0.3.

Loads and boundary conditions: Hydrostatic pressure of 2.01 MPa at outer surface of pipelines as the designed

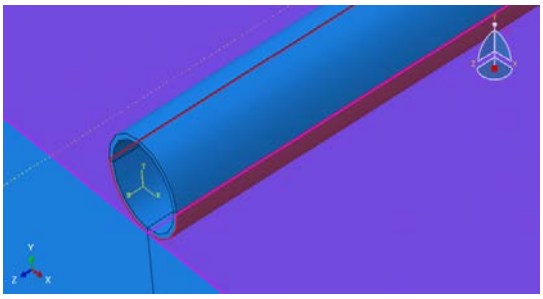

Fig. 3: Interaction of pipeline and seabed

Table 4: Summary of Abaqus modeling

Description	Intact pipeline	Defect pipeline	Seabed
3D deformable solid extrusion	√	√	√
Length of extrusion = 80.00 m	√	√	√
Outer diameter = 0.3556 m	√	√	
Cut-extrude parts: forming internal section of pipelines	√	√	
Cut-extrude-blind parts: forming designed corrosion part		√	

Table 5: Material properties of pipelines

Description	API 5L X42	API 5L X52	API 5L X65
Steel density (kg/m^3)		7850	
Young's modulus (GPa)		207	
Poison's ratio		0.3	
Thermal expansion coefficient (°C^{-1})	1.17×10^{-5}		
SMYS (MPa)	289	358	448
SMTS (MPa)	413	455	530

Table 6: Material properties of seabed

Description	Values
Wet clay density (kg/m^3)	1760
Young's modulus (GPa)	200
Poison's ratio	0.33
Cohesive yield stress (kPa)	100

water depth of pipelines located at 200 m underwater. Meanwhile the internal pipe's pressure of 6 MPa was input into internal pipe's surface. The selection of internal

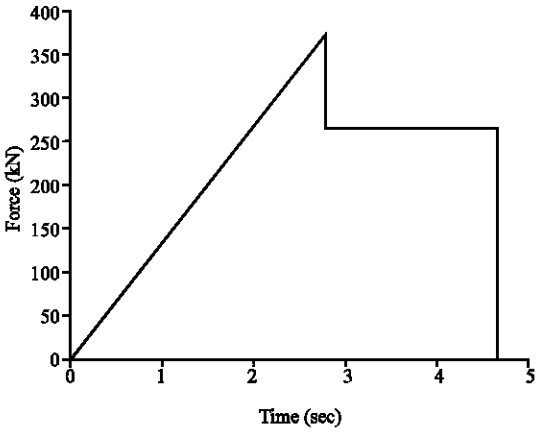

Fig. 4: Beam trawl pull-over duration

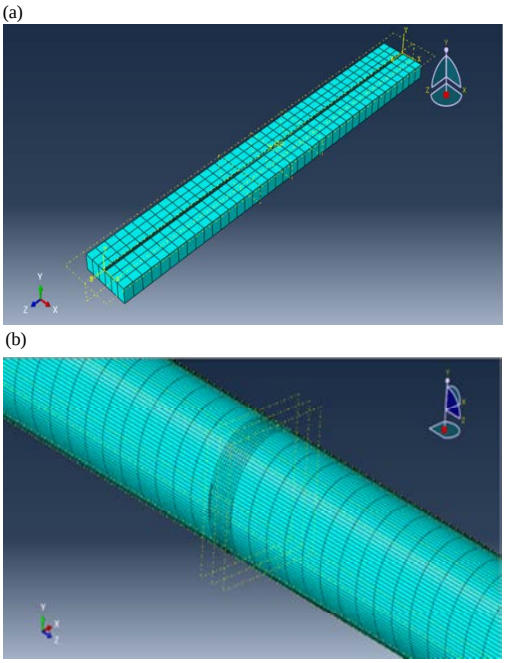

Fig. 5: Meshing of; a) Whole model and b) Pipeline corroded part

pipe's pressure was determined by the maximum allowable operating pressure among the steels. The designated internal pipe's pressure was approximate 14% lower than the lowest value of maximum allowable operating pressure among all steels to enable all simulation running before the pipeline bust.

Two point beam trawl forces applied as amplitude at a distance of 17.00 m equally from the center datum plane which is calculated based on DNV RP F111 as shown in Fig. 4. The seabed was not moveable and considered as rigid and non-deformable. Thus, it was set into fixed for the whole cell of seabed. For the pipeline, both pipe's end were fix to avoid movement at the pipe's end. It was the initial conditions that were designed for this study. The operating temperature of the fluid content inside the pipe was set to 120°C and the ambient temperature of pipe's surrounding condition was set to 5°C (Herlianto *et al*., 2012).

Meshing: The critical part of this model was situated at the corrosion defect region where the expected failure occurred. Therefore, a smaller meshing size has been applied to the defect pipe region compared to other region. The non-defect bodies of corroded pipe was refined by mesh size of 0.08 m and the corrosion defect region mesh size was further refined which is 0.01 m. Meanwhile, the seabed plays an insignificant role in the study as it focus on the pipeline changes. Therefore, the coarse mesh size of 2.00 m was selected for the seabed as shown in Fig. 5.

RESULTS AND DISCUSSION

Through the Eq. 2, the maximum allowable operating pressures were calculated for all cases as shown in Table 7. It can be seen that the maximum allowable operating pressure decrease with the increase of corrosion percentage for each type of steels, respectively.

A finite element analysis by using Abaqus/CAE 6.13-1 was done for five case study with varies on corrosion depth parameter with different type of materials which is case no corrosion, case 40% corrosion, case 50% corrosion, case 60% corrosion and case 70% corrosion. The analysis results were presented for each case study in term of lateral displacement, von Mises stress distribution and maximum principle strain distribution.

Lateral displacement: In observing the effect of beam trawl pull-over loads to the HT/HP subsea pipeline, lateral displacement of pipeline in relationship with time was analyzed as shown in Fig. 6. For all case except case 60% and 70% corrosion, two shrinking stage of lateral displacement in pipe was found when the pull-over forces reduced as per calculated according to DNV RP F110. Lateral buckling occurred after the pull-over duration was ended. The applied lateral load results in the formation of compression and tension in the pipeline section. In the bended pipe section, the compressive and tension continue to expand with the induced of surrounding water pressure that make the situation worsen. This theory was similar to lateral deflection of a flange.

In observing the lateral displacement induced by beam trawl pull-over forces along the pipe's length, the

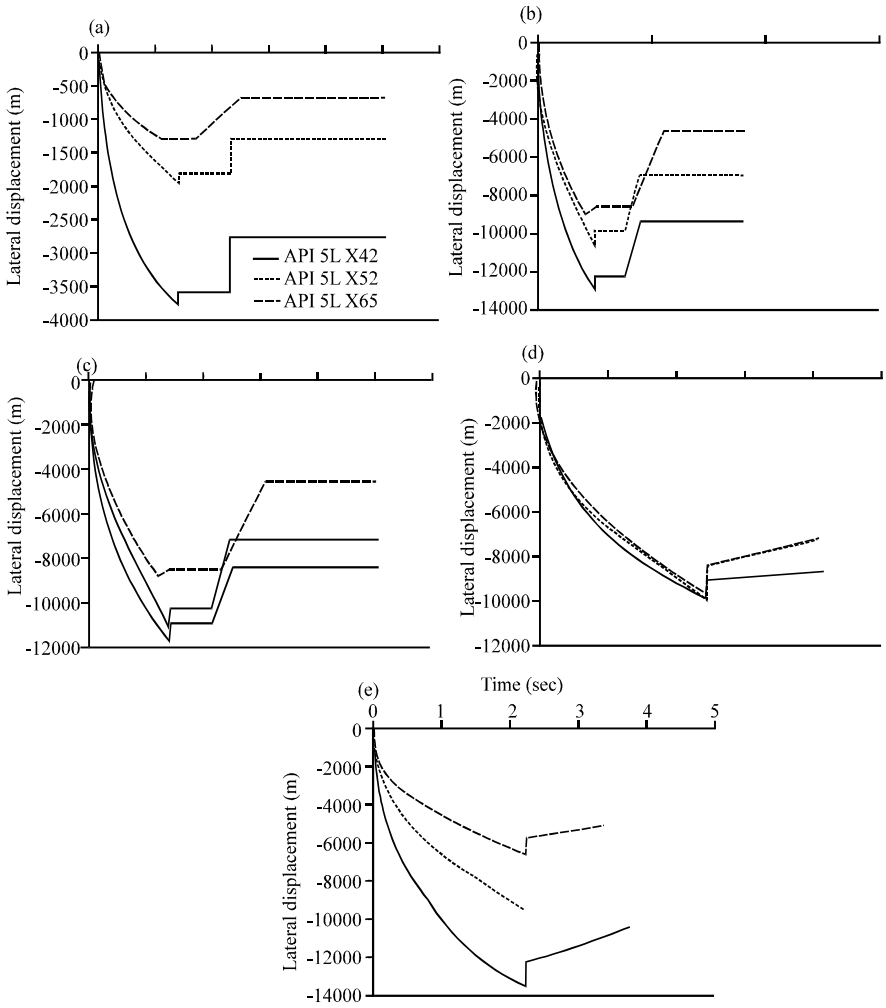

Fig. 6: Lateral displacement versus time for; a) Case no corrosion; b) Case 40% corrosion; c) Case 50% corrosion, d) Case 60% corrosion and e) Case 70% corrosion

Table 7: Maximum allowable operating pressure for all case studies

Case study	Pipeline material	Max allowable operating pressure (MPa)
No corrosion	API 5L X42	22.333
	API 5L X52	27.656
	API 5L X65	34.575
40% corrosion	API 5L X42	14.740
	API 5L X52	18.253
	API 5L X65	22.820
50% corrosion	API 5L X42	12.283
	API 5L X52	15.211
	API 5L X65	19.016
60% corrosion	API 5L X42	9.827
	API 5L X52	12.169
	API 5L X65	15.213
70% corrosion	API 5L X42	7.370
	API 5L X52	9.126
	API 5L X65	11.410

pipeline tends to deform laterally when the yield stress of the pipe materials exceeded. As the yield strength increases from API 5L X42, API 5L X52-API 5L X65, the lateral displacement also increase from API 5L X42, API 5L X52-API 5L X65. The graph trends are occurred almost all case except case 60 and 70% corrosion. It can be conclude that case 40 and 50% corrosion exhibit similar behavior when exerted beam trawl pull-over forces as shown in Fig. 7b and c. A different graph trend can be observed for cases 60 and 70% corrosion with other cases as shown in Fig. 7d, e. This is because part of the pipe after 40.00 m was perforated into seabed, therefore, the soil resist further lateral displacement of pipes while the unburied pipe keep on moving laterally, creating uneven lateral displacement in a pipeline.

Von Mises stress: As the both pipe's end are fixed, therefore, it is reasonable for having highest von Mises

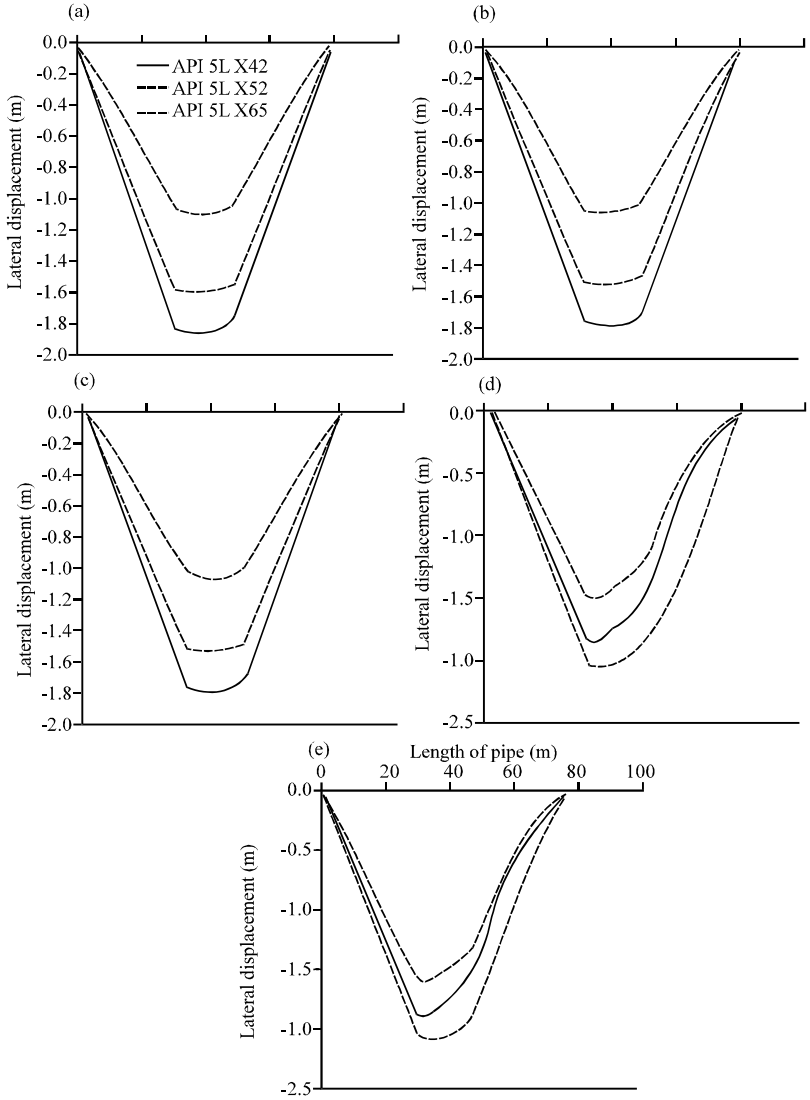

Fig. 7: Lateral displacement versus length of pipe for; a) Case no corrosion; b) Case 40% corrosion; c) Case 50% corrosion; d) Case 60% corrosion and e) Case 70% corrosion

stress distributions on both pipe's end where material with lowest tensile strength would have the highest von Mises stress. At the trawling point, the pipeline buckles into a series of sinusoidal half waves with different buckle amplitudes due to the difference in materials used in pipeline. Thus, it has noticeable highest von Mises stress for API 5L X42 at trawling point followed by API 5L X52 and API 5L X65. At before and after the trawling point, there was a subsequent increase in von Mises stress for all materials due to high resistance of materials for buckling in pipe at the both trawling points. It was recorded the highest for API 5L X52 as it had the highest ductility properties. At the corrosion defect area, API 5L X52 ranked the highest von Mises stress among all materials. A similar graph trend for cases 40 and 50% corrosion was noticed as shown in Fig. 8b, c. It showed a diverse graph trend for case 60 and 70% corrosion with case no corrosion, case 40% corrosion and case 50% corrosion. The final simulation result for cases 60 and 70% corrosion were found that parts of the pipeline after 40.00 m has been perforated into seabed as shown in Fig. 8d, e. Therefore, the pipeline buckling was stopped when it reach a maximum restriction in seabed.

Maximum principle strain: At the trawling point, it recorded the highest strain where the beam trawl hooks on pipe for very short period creates high forces on those

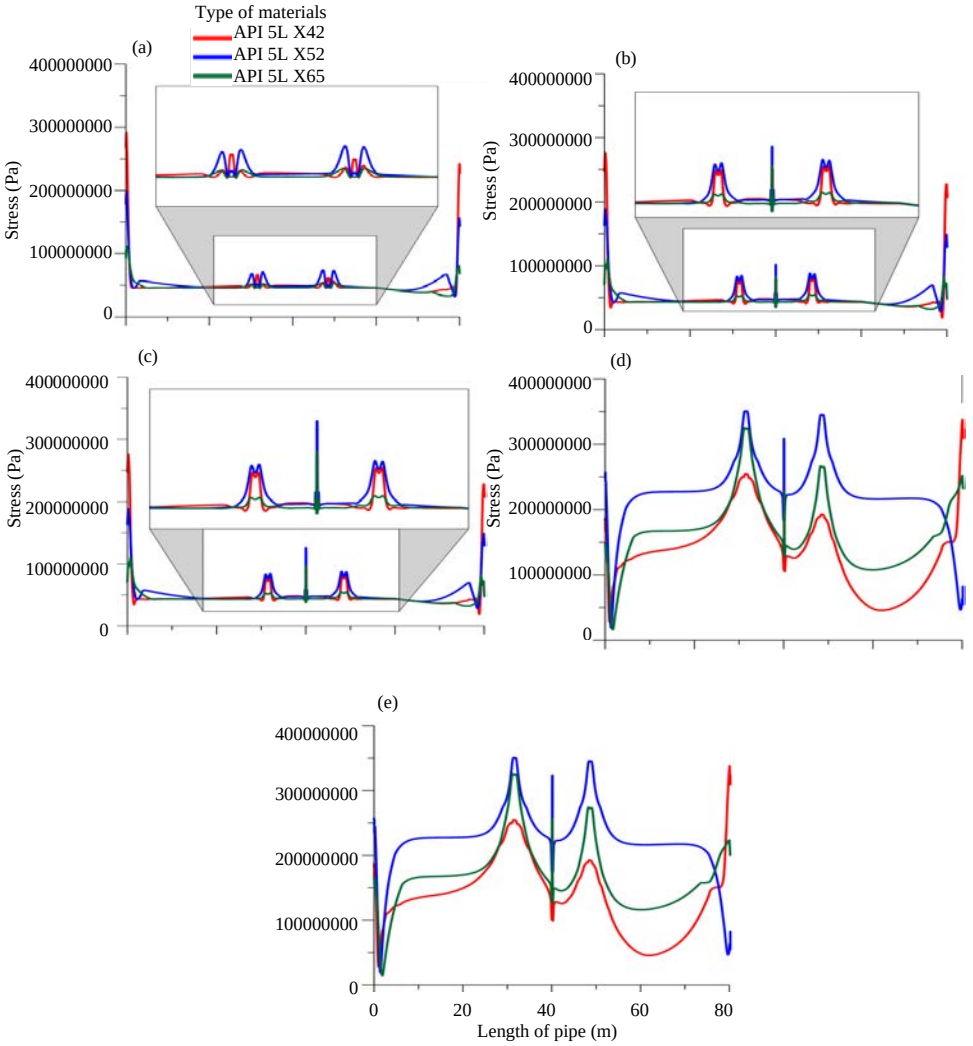

Fig. 8: Stress versus length of pipe for; a) Case no corrosion; b) Case 40% corrosion; c) Case 50% corrosion; d) Case 60% corrosion and e) Case 70% corrosion

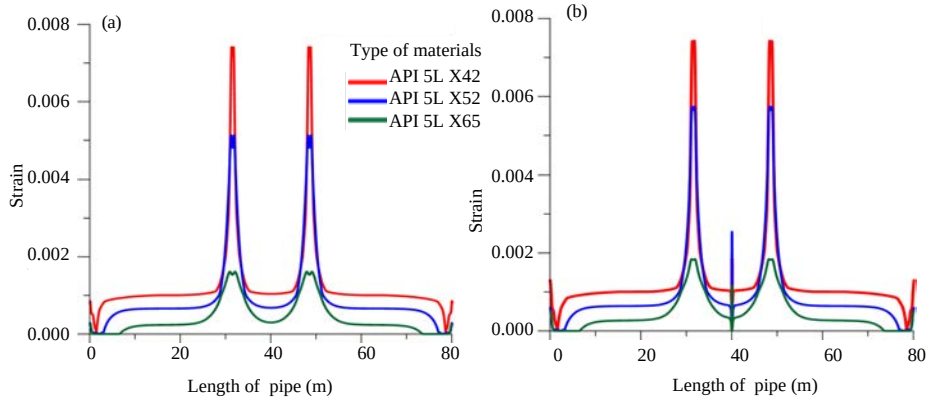

Fig. 9: Continue

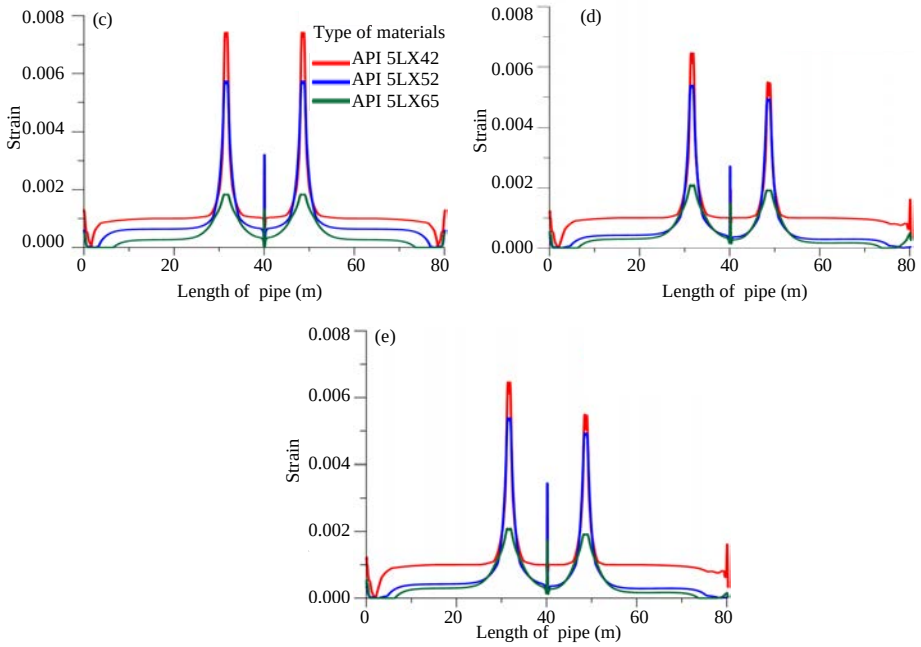

Fig. 9: Strain versus length of pipe for; a) Case no corrosion; b) Case 40% corrosion; c) Case 50% corrosion, d) Case 60% corrosion and e) Case 70% corrosion

pipe sections. It was occurred in all cases for highest strain at the trawling points. At the corrosion defect at 40 m of pipe, it observed that API 5L X52 had the highest strain followed by API 5L X42 and API 5L X65. It is coincide with the von Mises stress results at the corrosion defect area. The same trend can be observed except it had higher strain at corrosion defect area than of case 40% corrosion as shown in Fig. 9b and c. An almost similar trend for case 60 and 70% corrosion at trawling point as shown in Fig. 9d, e can be observed with case 40% corrosion and case 50% corrosion strain-length of pipe graphs except the strain at 48.5 m trawling point was lower than of 31.5 m trawling point. It was resulted as the pipe after 40.00 m was perforated into the seabed.

CONCLUSION

In this study, it was attempted to study the beam trawl force and lateral bucking behavior on a corroded pipeline in different type of steel grade. It can be concluded that lateral buckling pipeline was induced slightly after the beam trawl forces is zero after 4.628 sec. In term of materials used in pipelines, the tensile strength increases from API 5L X42-52 and follow by API 5L X65. Increasing tensile strength resulted in higher shrinking ability after the beam trawl pull-over forces for API 5L X65 pipeline

When corrosion in term of depth parameter was been investigated on beam trawl pull-over HT/HP pipelines, the case study had shown similarity behavior on von Mises stress, strain and lateral displacement between case 40 and 50% corrosion as well as between case 60 and 70% corrosion along length of pipeline.

For the displacement controlled condition buckling code check of DNV OS F101 for case study was carried out, it was found that all cases are application to the buckling code check except case 60 and 70% corrosion which means that it was not susceptible for buckling to occur. This is proven to be same as the FEA simulation analysis as the simulation had stopped before it can be buckled for case 60 and 70% corrosion.

RECOMMENDATIONS

Further studies should be carried out with different dimension of pipeline, variation on temperatures, pressures and materials to have a better conclusion. Other than that, mesh convergence studies with finer mesh size are encouraged for a more precise and accurate results that closer to real life situations. The seabed should be considered for taking real bathymetry based on actual locations including spans and type of soils. Other than that, flow analysis was also suggested in investigated this research.

NOMENCLATURE

ASME = American Society of Mechanical Engineer
API = American Petroleum Institute
DNV = Det Norske Veritas
FEA = Finite Element Analysis
OOS = Out-of-Straightness
OS = Offshore Standard
RP = Recommend Practice
SMYS = Specified Minimum Yield Stress
3D = Three Dimension

REFERENCES

Anonymous, 2007. Global buckling of submarine pipelines structural design due to high temperature/high pressure: DNV recommended practice RP -F110. DNV GL., Oslo, Norway.

Anonymous, 2010a. Interference between trawl gear and pipelines: DNV recommended practice RP-F111. DNV GL., Oslo, Norway.

Anonymous, 2010b. Risk assessment data directory: Risers and pipeline release frequencies. OGP UK., England, UK.

Anonymous, 2013. Submarine pipeline systems: DNV offshore standard OS-F101. DNV GL., Oslo, Norway. http://rules.dnvgl.com/docs/pdf/DNV/codes/docs/2013-10/OS-F101.pdf

Guo, L.P., R. Liu and S.W. Yan, 2013. Low-Order Lateral Buckling Analysis of Submarine Pipeline under Thermal Stress. In: New Frontiers in Engineering Geology and the Environment, Huang, Y., F. Wu, Z. Shi and B. Ye (Eds.). Springer, Berlin, Germany, ISBN:978-3-642-31670-8, pp: 191-194.

Herlianto, I., Q. Chen and D. Karunakaran, 2012. Lateral buckling induced by trawl gears pull-over loads on high temperature/high pressure subsea pipeline. Proceedings of the ASME 2012 31st International Conference on Ocean, Offshore and Arctic Engineering, July 1-6, 2012, American Society of Mechanical Engineers, Rio de Janeiro, Brazil, ISBN:978-0-7918-4490-8, pp: 235-240.

Khair, A.J., K. Jaswar and A.A.F. Effendi, 2015. Buckling criteria for subsea pipeline. J. Teknologi, 74: 69-72.

McAllister, E.W., 2013. Pipeline Rules of Thumb Handbook: A Manual of Quick, Accurate Solutions to Everyday Pipeline Engineering Problems. Elsevier, New York, USA., ISBN:978-0-12-387693-5, Pages: 792.

Montgomerie, M., 2011. Gear technology Note-towed gear. Sea Fish Industry Authority, UK. http://www.seafish.org/media/Publications/SeafishGuidanceNote_TowedGear_201102.pdf